ILMATIETEEN LAITOS
METEOROLOGISKA INSTITUTET
FINNISH METEOROLOGICAL INSTITUTE

RAPORTTEJA
RAPPORTER
REPORTS
2011:8

THE RADIATION, SNOW CHARACTERISTICS AND ALBEDO AT SUMMIT (RASCALS) EXPEDITION REPORT

AKU RIIHELÄ
PANU LAHTINEN
TEEMU HAKALA

RAPORTTEJA
RAPPORTER
REPORTS
2011:8

The Radiation, Snow Characteristics and Albedo at Summit (RASCALS) expedition report

Aku Riihelä (1), Panu Lahtinen (1), Teemu Hakala (2)

(1) Ilmatieteen Laitos & (2) Geodeettinen Laitos
(1) Finnish Meteorological Institute & (2) Finnish Geodetic Institute

Ilmatieteen laitos
Meteorologiska Institutet
Finnish Meteorological Institute

Helsinki, 2011

ISBN 978-951-697-759-4 (nid.)
ISBN 978-951-697-760-0 (pdf)
ISSN 0782-6079

Unigrafia
Helsinki 2011

ILMATIETEEN LAITOS

Julkaisun sarja, numero ja raporttikoodi
Raportteja 2011:8

Julkaisija Ilmatieteen laitos
(Erik Palménin aukio 1)
PL 503
00101 Helsinki
Julkaisuaika 2011

Tekijät
Aku Riihelä, Panu Lahtinen, Teemu Hakala

Projektin nimi

Tilaaja
Ilmatieteen laitos

Nimeke
Radiation, Snow Characteristics and Albedo at Summit (RASCALS)-retkikunnan kenttäraportti

Tiivistelmä
RASCALS-retkikunnan tehtävä oli tutkia Grönlannin mannerjäätikön lumen fysikaalisia ja optisia ominaisuuksia sekä Auringon valon vuorovaikutusta lumen kanssa. Retikunta vietti hieman yli kolme viikkoa mannerjäätikön keskellä sijaitsevalla Summit Camp-tutkimusasemalla tehden mittauksia. Sääolot suosivat kampanjaa, jonka seurauksena onnistuttiin keräämään laaja ja monipuolinen tietoaineisto mannerjäätikön lumen pintakerroksesta ja eritoten lumen heijastavuuden (albedon) käyttäytymisestä. Aineisto on hyödyllinen kehitettäessä ja varmennettaessa lumen albedon kaukokartoitusmenetelmiä satelliiteilla.

Julkaisijayksikkö
Uudet Havaintomenetelmät (UHA)

Luokitus (UDK)
528.8, 551.32, 550.3, 551.52

Asiasanat
Jäätiköt,albedo, lumi,
kaukokartoitus, lumen fysiikka,
Grönlanti

ISSN ja avainnimike
0782-6079 Raportteja - Rapporter - Reports

ISBN
ISBN 978-951-697-759-4 (nid.)
ISBN 978-951-697-760-0 (pdf)

Kieli
Englanti (tiivistelmä suomeksi)

Myynti
Ilmatieteen laitos
PL 503
00101 Helsinki

Sivumäärä 48

Hinta

Lisätietoja

FINNISH METEOROLOGICAL INSTITUTE

Series title, number and report code
of publication
Reports 2011:8

Published by Finnish Meteorological Institute
(Erik Palménin aukio 1)
P.O. Box 503
FIN-00101 Helsinki, Finland Date 2011

Author(s)
Aku Riihelä, Panu Lahtinen, Teemu Hakala

Name of project

Commissioned by
Finnish Meteorological Institute

Title
The Radiation, Snow Characteristics and Albedo at Summit (RASCALS) expedition report

Abstract
The RASCALS expedition spent over three weeks at the Summit camp research station near the top of the Greenland Ice Sheet during polar summer 2010. During this time, detailed measurements of the physical and optical properties of Arctic perennial snow were carried out concurrently with snow albedo and reflectance measurements. Favorable weather conditions during the campaign enabled the collection of a large dataset on Arctic snow albedo and associated quantities for use in developing and validating remote sensing algorithms for snow albedo using satellites. This report provides a description of the measurements and conditions during the campaign.

Publishing unit
Earth Observation (UHA)

Classification (UDK)
528.8, 551.32, 550.3, 551.52

Keywords
Glaciers,albedo, snow,
remote sensing, snow physics,
Greeland

ISSN and series title
0782-6079 Raportteja - Rapporter - Reports

ISBN
ISBN 978-951-697-759-4 (nid.)
ISBN 978-951-697-760-0 (pdf)

Language
English (abstract also in Finnish)

Sold by
Finnish Meteorological Institute
P.O.Box 503
FI-00101 Helsinki, Finland

Pages 48 Price

Note

Contents

Chapter 1

Introduction

The cryosphere of the Earth is one of the most important components of its climate system. Snow cover of the Northern Hemisphere extended annually to over 45 million square kilometers in January during the years 1972-1992 [1]. In terms of radiation physics, snow is completely different from vegetated terrain or bare soil; Snow reflects anywhere between 50 and 90 per cent of incoming Solar radiation depending on its characteristics. This high reflectivity, or albedo, is one of the key drivers of the radiation budget of the Northern Hemisphere. The radiation budget ultimately governs the solar energy absorbed in the Earth's climate system. To understand its state and the evolution, we need to develop means to effectively and reliably monitor the albedo of snow.

There are numerous obstacles in monitoring the snow albedo and other radiation characteristics. The Arctic regions are remote, sparsely populated and their environment is unforgiving. Observations of the radiative processes in and over the snow cover for climate research and monitoring applications require sustained long-term surveillance of the entire Arctic (and Antarctic) regions. This requirement renders in situ observations from, e.g. weather stations or airborne radiation sensors insufficient. Spaceborne observations from satellites are the most practical means of achieving hemispherical coverage with long-term surveillance capacity.

Unfortunately, even the most sophisticated satellite radiation sensors cannot observe snow albedo directly. Snow albedo is defined as the total fraction of incoming radiation reflected by a snow surface to all directions in the incident radiation's hemisphere (i.e. the sky). A satellite can only ever observe the reflected radiation from a single direction. Knowing that snow is typically a very strong anisotropic scatterer of light [2], we find the necessity of performing comprehensive field campaigns of snow studies to validate and further develop the methods designed to derive the actual snow albedo from the limited satellite observations. Also, knowledge on the interdependencies of the albedo and physical characteristics of snow is crucial for assessing the robustness and global applicability of current satellite-based snow albedo products.

This report describes the expedition undertaken by Finnish Meteorological Institute (FMI) and Finnish Geodetic Institute (FGI) researchers to the Greenland Ice Sheet during polar summer 2010 to study the albedo and relevant physical properties of pristine Arctic snow. The observed datasets, instruments used, as well as prevailing environmental conditions will be reported.

Chapter 2

Campaign Description

2.1 Campaign Objectives

The RASCALS campaign was designed to achieve the following goals:

- To gather datasets on the broadband albedo, directional reflectance and physical properties of pristine Arctic snow.
- To study the connections and dependencies between the physical and radiative properties (e.g. albedo or directional reflectance) of snow.
- To specifically gather clear-sky datasets on snow albedo and directional reflectance for use in the validation of satellite-based snow albedo products.

2.2 Campaign Dates and Location

The RASCALS campaign took place between June 28 - July 21, 2010 at Summit Environmental Observatory (herewith Summit station) on the top of the Greenland Ice Sheet (GIS). The geographical coordinates of the station are 72°35'46.4" N, 38°25'19.1" W. The station location is illustrated in Figure 2.1. The station is located on the accumulation zone of the ice sheet, meaning that there is a annual net gain of snowpack depth. Due to its height (at 3200 m a.s.l.), the temperatures do not reach above 0 °C even during mid-summer. Thus, the snow does not experience significant melting.

Summit station was chosen as the expedition target for the following reasons. First, Summit station is extremely remote, being located over 400 km from the nearest human habitation. The snow on site is both completely untouched and also has a very low impurity concentration from anthropogenic sources. Secondly, Summit station possesses a good infrastructure for supporting field expeditions. The station staff provides tent accomodations and provisions for all visiting researchers, making expedition logistics considerably simpler. The station also provides snow mobiles and sleds to researchers upon request and usage-based reimbursement. This enables the expedition to cover a larger area around the station with measurements. The station also has heated mechanic shops and limited heat storage space for sensitive scientific equipment. An overview photograph of the station area is shown in Figure 2.2.

Access to Summit station is negotiated with the U.S. National Science Foundation (NSF). Upon acceptance of expedition application, the research PI needs then to form an agreement with CH2M Hill Polar Services Inc., which is responsible for the operations on site. Due to the harsh environment and high altitude, all expedition members are required to undergo a comprehensive medical examination. In addition to the basic per-day user costs and transportation costs to and from the station, the expedition may request on site mechanics or science technicians to assist with the measurement on an availability and per-cost basis.

Transportation to the station is arranged through the New York Air National Guard. The C-130 Hercules military transport planes ferry staff and cargo between the station and the Kangerlussuaq

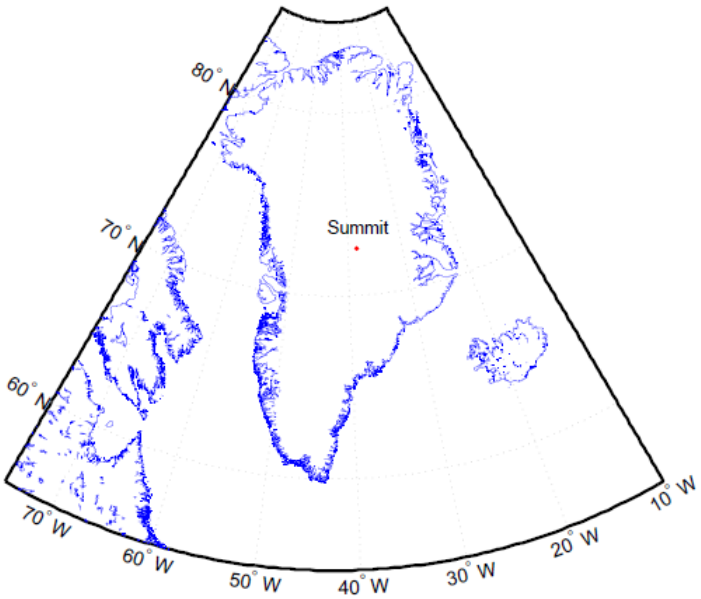

Figure 2.1: The location of Summit station.

Figure 2.2: Overview of Summit station area. Front: tent city for visiting researcher. Back, middle part: Big House, the kitchen and social area of the station. On the right: The Shop, mechanics and storage area.

air port. Kangerlussuaq is reachable by commercial air (Air Greenland) from Copenhagen. Commercial cargo handling companies (for example DHL) may be contracted to handle the transportation of scientific and personal equipment shipments to the Polar Services offices in Kangerlussuaq. Expedition staff is requested to arrive to Kanger at least a day in advance to the scheduled transport to Summit. Polar Services offers accomodations and meals at Kanger during the transport wait period. Expedition PIs should note that poor weather conditions may delay the air transport up to several days.

2.3 Measured Quantities and Measurement Instrumentation

The objective of RASCALS was to measure concurrently all the snow characteristics relevant to its albedo, with the exception of snow impurities content, which is typically negligible at Summit.

During the campaign, the radiative and physical quantities in table 2.1 were measured using the instruments listed.

Quantity	**Instrument**
Broadband surface albedo	Kipp & Zonen CM-14
Spectral nadir reflectance and irradiance	ASD FieldSpec 3
Hemispherical-directional snow reflectance (BRF)	FIGIFIGO spectrogonioradiometer
Snow temperature at 5-10 cm depth	FLUKE 1524
Snow temperature profile	Thermometer
Snow density profile	250cc Snowmetrix RIP 2 cutter + digital scale
Snow crystal photographs	Canon 450D + 60/2.8 Canon EF-s macro with extension
Snow permittivity	Toikka Snow Fork
Snow temperature profile time-series	T-log temperature logger
Brightness temperature of snow surface	IR thermometer
Light extinction in snowpack	SPAM* snow measurement unit
Day-time snow grain evolution in top 30cm of snowpack	Canon 450D + 60/2.8 Canon EF-s macro with extension
Snow surface roughness incl. day-time evolution	Graded plate + Canon G-10
Snow profile NIR photographs	modified Canon 350D + 18-55 lens
Basic weather conditions (wind dir, cloudiness, etc.)	Skywatch Xplorer 4 + compass + visual observation

Table 2.1: The observed quantities and the instruments used. (*) SPAM is short for Snow Profile Associated Measurements.

Since some of the instrumentation is custom-built for FMI snow research, we shall also briefly introduce the instrumentation where they differ from off-the-shelf equipment.

2.3.1 Finnish Geodetic Institute Field Goniometer (FIGIFIGO)

Finnish Geodetic Institute Field Goniospectrometer (FIGIFIGO) an instrument designed for multiangular reflectance factor measurements, known as bidirectional reflectance factor (BRF) and

hemispherical directional reflectance factor (HDRF) [3]. These measurements are taken by moving a sensor head around a target, which is in the center of the measurement hemisphere. FIGIFIGO can be operated both on field under sunlight conditions (HDRF), and in laboratory using artificial illumination (BRF). The instrument design is primarily for field operation, as the total weight of the system has been kept as low as possible, at around 40kg, and all critical components are designed to withstand field conditions. The instrument is highly automated and needs to be operated by two persons during summer. During winter only one operator is needed, as it can easily be slided on snow. Instrument setup is fast, only about 5-15 minutes, depending on how it was packed. After initial setup moving to a nearby sample takes only few minutes. A typical measurement of full hemisphere (200-400 spectra) takes about 15 minutes after setup. The FIGIFIGO instrument in measurement configuration at Summit is illustrated in Figure 2.3. The small size of the instrument is evident.

Figure 2.3: The FIGIFIGO instrument in measurement configuration with operator.

The primary instrument of FIGIFIGO is an ASD FieldSpec Pro FR optical fiber spectroradiometer (350-2500 nm), which is housed inside a rugged casing along with lead acid batteries, electronics and an electric motor. The motor is used to drive a telescopic measurement arm (1.55-2.65 m) from vertical to $\pm$ 90°for the zenith angle adjustment. The azimuth angle is adjusted by turning the whole device around the sample. The sample is viewed by downward looking optics mounted to the top of the measurement arm and the optics are connected to the spectroradiometer by a 3 meter optical fiber. In addition to regular optics, a set of polarizing optics have been constructed using a Glan Thompson polarizer inside a rotator. The polarizing optics can be used to measure the sample with two or more polarization directions. The whole system is controlled by LabVIEW control software running in a rugged laptop.

The measurement starts by first choosing a representative 0.5 m diameter sample of the target surface. FIGIFIGO is positioned next to the sample and calibrated for current illumination conditions (spectrometer optimization and white reference) using a 99% reflective Labsphere Spectralon 25x25 cm^2 reference panel. At this point the system measures the current GPS position and time, and calculates the sun zenith and azimuth angles. FIGIFIGO uses a hemispherical (fish eye) camera to measure the direction of the measurement plane relative to the sun direction (sensor azimuth direction). Inclinometer is used to measure the zenith angle of the measurement arm (sensor zenith direction). The sample surface is measured at several azimuth directions by moving FIGIFIGO around the sample, and simultaneously a silicon pyranometer is used to measure the illumination conditions, clouds, haze, and other atmospheric disturbances. During sunlit measurements the diffuse illumination from sky and surroundings is measured at by first shadowing the sample (blocking only direct solar direction) and then measuring a spectrum from the shadowed target. This diffuse illumination is also measured for the Spectralon panel. After the measurements the data needs to be processed by Matlab software that takes in all the sensor data, does interpolations to match the spectra and the direction data, calculates BRF from the measured HDRF data using

the diffuse measurements, corrects the spectra with the pyranometer data, and then outputs the data to a library format for easy processing. The library format has each measured spectrum with UTC time and direction information.

2.3.2 Albedometer and spectrometer

The instrument we used to record the shortwave broadband albedo of snow at Summit was an off-the-shelf Kipp & Zonen CM-14 albedometer, consisting of two back-to-back CM-11 pyranometers. The unit was calibrated against reference pyranometers at FMI during 2009 and 2011, so it's accuracy may be assumed to be well within manufacturer specifications. The CM-14 is defined as a "secondary standard" quality instrument according to ISO 9060 specification. Its wavelength sensitivity range is defined as 310-2800 nm (containing 50% of points). The accuracy of the albedometer observations will be discussed in section 3.2.5. The albedometer is shown in measurement configuration at Summit in Figure 2.4.

Figure 2.4: The CM-14 albedometer in measurement configuration at Summit.

The spectrometer used for spectrally resolved irradiance measurements and nadir snow reflectance measurements was an off-the-shelf ASD FieldSpec 3. The FieldSpec 3 is sensitive to radiation in the waveband of 350-2800 nm, with spectral resolution between 3 and 8.5 nm depending on the observed wavelength. Irradiance measurements were made with the RCR (remote cosine receptor) foreoptic. Snow nadir reflectance observations were made with the standard 8-degree foreoptic with pistol grip, both provided by ASD. The 8-degree was chosen over the 1-degree to gain a somewhat larger footpring on the snow surface and thus minimize any geometrical shadowing effects on the reflectance. The foreoptic was mounted on a tripod at approximately 1 meter height for irradiance observations and approximately half a meter for the snow reflectance. The tripod was lowered to ensure that the Spectralon calibration reference used would fill all of the instrument's FOV. Again, the accuracy of these measurements will be discussed in section 3.2.5.

2.3.3 T-log temperature logger

To record the diurnal cycle of the snow temperature, a custom thermometer logger was constructed. The logger consists of a PVC plastic tube with eight Dallas Semiconductor DS18S20 1-Wire thermometer sensors and one Melexis MLX90614ESF-AAA infrared thermometer. Six sensors were placed so that the temperature of the surface layer was measured with 2 cm increments from surface down to 10 cm and one at 20 cm below the surface and one 5 cm above the surface. The IR-sensor is located 25 cm above the surface and aligned to view snow surface at a distance of approximately

50 cm away of the vertical tube so that shadowing would not affect the measurement. The logger unit consists of a Arduino Duemilanove microcontroller board with GPS data logger.

2.3.4 Snow Profile Associated Measurements (SPAM)

SPAM-instrument is a prototype of a new instrument concept for snow profiling (temperature, snow layering, light extinction). The instrument consists of a 1.2 meter long shaft with sensors at the lower end, and processing unit with ultrasonic range detector at the top, which is used as depth reference. The sensors used in this prototype were Melexis MLX90614ESF-AAA infrared thermometer and TAOS TSL230R irradiance sensor.

The first tests of the instrument were made during the RASCALS expedition. The first results and characterization of SPAM is reported in [4].

2.3.5 Near-Infrared snow crystal camera

Near-infrared (NIR) images of the snow profile were taken to reveal the snow layering and to make an estimate of the snow specific surface area. Time-constraints and the greater need of basic measurements of snow properties reduced the number of acquired images. The used camera is a modified Canon 350D with a 18-55 mm zoom lens. The modification to the otherwise standard digital single-lens reflex camera is the replacement of the near-infrared-blocking filter on the sensor to a NIR-pass filter (lets through near-infrared light, but blocks the visible portion).

2.3.6 Snow surface roughness

Snow surface roughness data were collected using a graded plate with known-sized grids at the border and a camera. The plate was inserted to snow so that most of it remained above the surface. By photographing this setup, the images can be rectified and the clear contrast difference between the black background of the plate and the snow-air interface can be found. From this the surface roughness parameters can be calculated. After quality control (removal of out-of-focus images and images with disturbed snow surface) 370 profiles remain.

2.3.7 Auxiliary data, courtesy of Summit station staff

In addition to the measurements performed by the expedition crew, the regular Automatic Weather Station (AWS) measurements from Summit station have also been made available for use, along with radiosonde observations of the lower atmosphere. In addition, data from the Greenland Climate Network (GC-Net) [5] AWS at Summit containing also radiative measurements have been requested but were not yet available at the time of writing this document. These data are not owned by the RASCALS expedition, but they are listed here for informative purposes.

The available AWS measurements from Summit station over the period of the campaign (21.6.-16.7.2010) are:

- Wind speed at 10m
- Wind direction at 10m
- Surface pressure
- Relative humidity at 2m
- Temperature at 2m
- Temperature at 10m

The radiosonde observations of the atmosphere at Summit station were a routine part of station operations over the period of the campaign (26.5. - 18.7.2010). Two atmospheric profiles per day were measured (1130 and 2330 UTC). The observed variables were:

- Height

- Air pressure
- Air temperature
- Dew point
- Relative humidity

Chapter 3

Campaign Data Description

3.1 Weather conditions during the campaign

We begin the campaign data description with an overview of the ambient weather conditions at Summit station. The air temperature at 2m, Wind speed at 10m and wind direction at 10m between 21.6. - 16.7.2010 are illustrated in Figure 3.1. The temperatures at Summit were typical of the season; daytime high was usually around -10 °C, with a nighttime low of -20 to -25 °C. Cloudiness increased substantially towards the end of the campaign (14.7. onwards), leading to an increase in air temperatures.

The wind speeds were also typical of the location and season. We recorded gust highs of ≈ 15 m/s near the end of the campaign. An unusual feature in the winds was the unusually high occurrence of northerly winds. Typical summer winds at Summit are from the southerly directions. The clean-air zone preservation conditions on site require that no engines be operated during north winds conditions except for purposes of vital station maintenance. Thus, the frequent north winds also limited our capability to perform off-station measurements. Fortunately, clean snow zones also existed close to the station.

The air and snow temperatures were also measured using the custom-built T-log temperature logging instrument. We show here the temperatures measured at 5cm height above the snow surface versus the 2m air temperature measured by the AWS at Summit. The data is shown in Figure 3.2. The data shows that the heating effect of the Sun on the T-log instrument chassis is considerable, even though the chassis was made of plastic. During night-time when the Sun is too low to have any significant energy input to the surface, we see a much better agreement between the instruments. The reason why the discrepancy is higher during the first half of the campaign is that we at first did not shield the T-log sensors from direct sunlight, then we experimented with some different ways of shielding the instrument with walls of packed snow.

In addition to the air temperature, the T-log also recorded temperatures inside the snow pack at 2, 4, 6, 8, 10 and 20 cm depths. In Figure 3.3, we show the measured snowpack temperatures at 10 and 20 cm below the snow surface. The data shows the delayed sine wave cycle of snow pack temperature as expected from theory. Also, the temperature variation is stronger nearer the surface, where the Solar insolation is stronger.

The Summit station science technicians also provided us with the radio sonde observations made during the campaign period. The radio sonde data records

- Height
- Pressure
- Temperature
- Dew point
- Relative Humidity

We show the air temperature profiles over Summit vs. height for the campaign period in Figure 3.4.

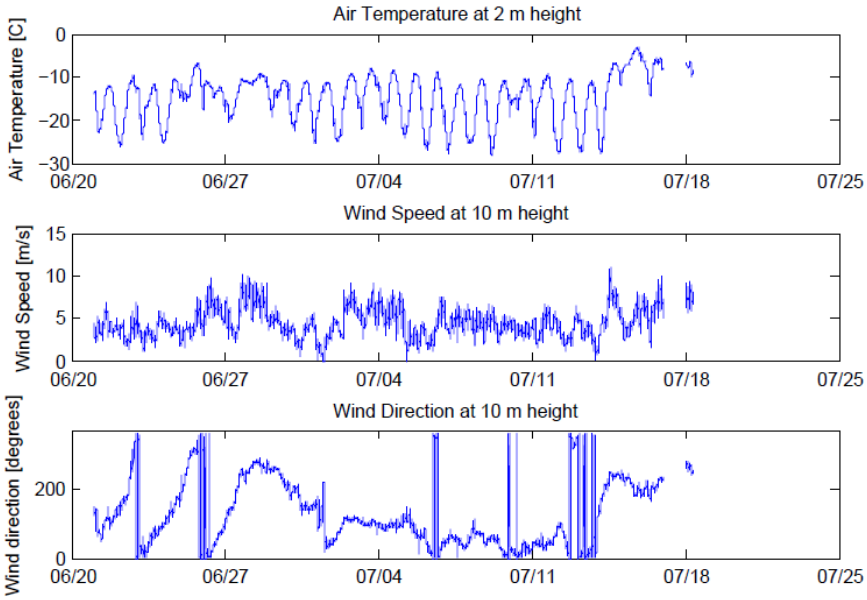

Figure 3.1: From top to bottom: Air temperature at 2m height, Wind speed at 2m height, and wind direction at Summit during the RASCALS campaign

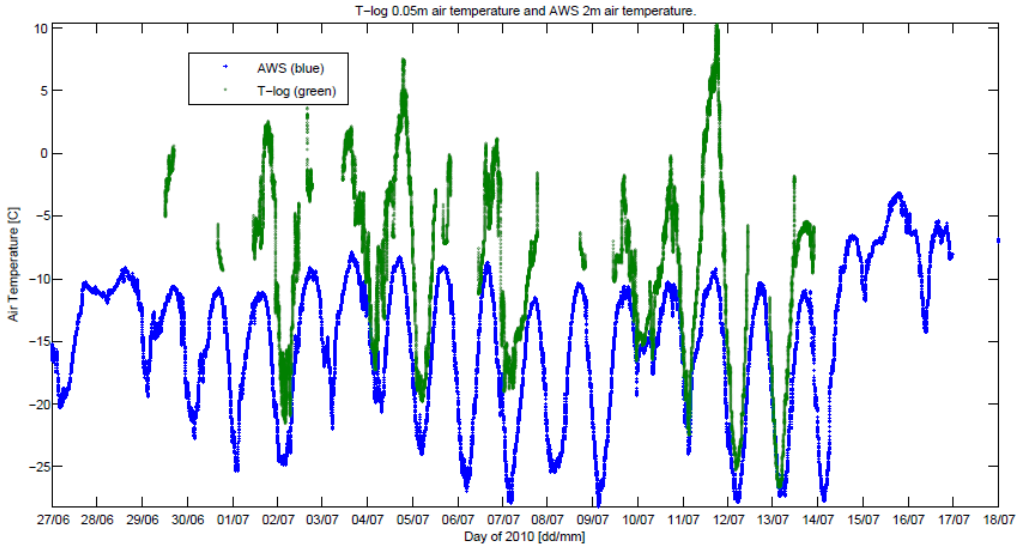

Figure 3.2: The air temperatures measured by the T-log instrument at 5cm height and the AWS and 2m height.

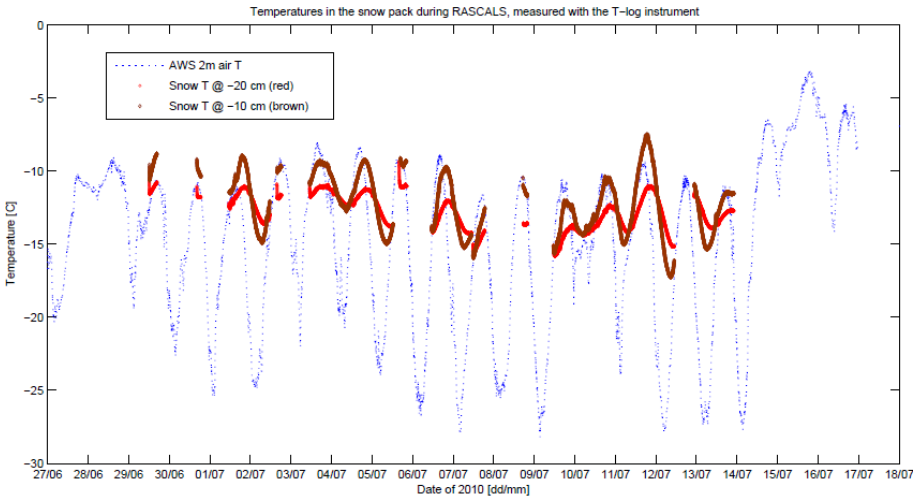

Figure 3.3: The temperatures inside the snowpack at 10 and 20 cm depth, measured by the T-log instrument. The AWS air temperature at 2m height is shown as reference.

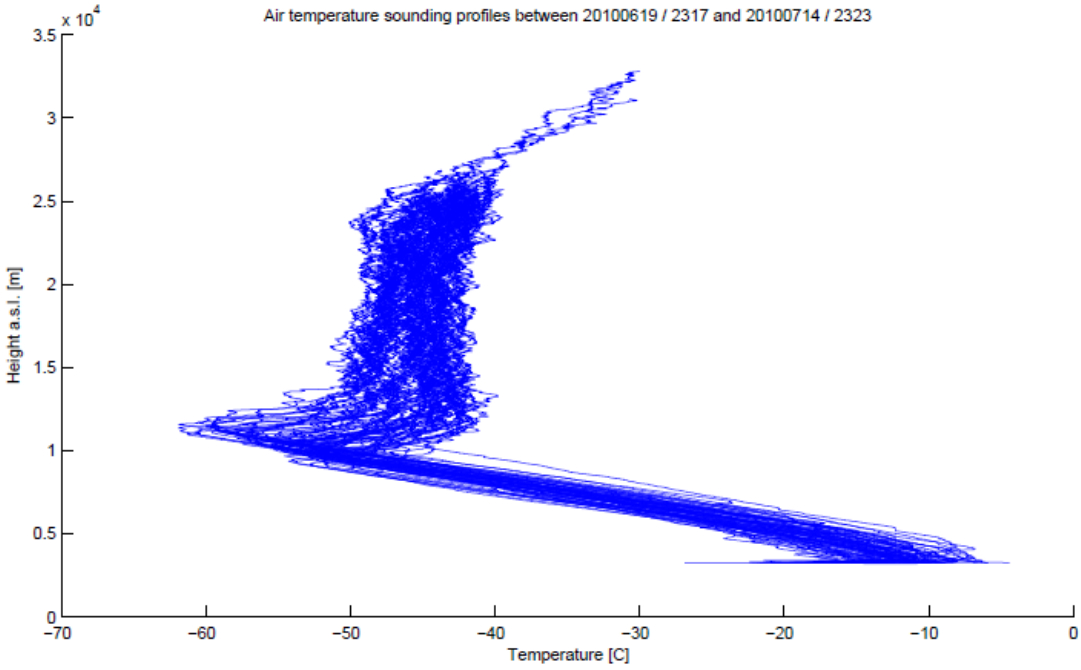

Figure 3.4: Air temperature profiles from radiosonde soundings performed by the Science tech staff of Summit station. All data is property of NSF and NOAA.

3.2 Observed radiative quantities

The observations of RASCALS took place between June 29 - July 16, 2010. Snowmobile availability at station enabled the expedition to also observe the snow away from station, thus ensuring that no contamination had occurred. The locations visited during RASCALS are illustrated in Figure 3.5. In the following sections, we will describe the radiative measurements according to measured variable.

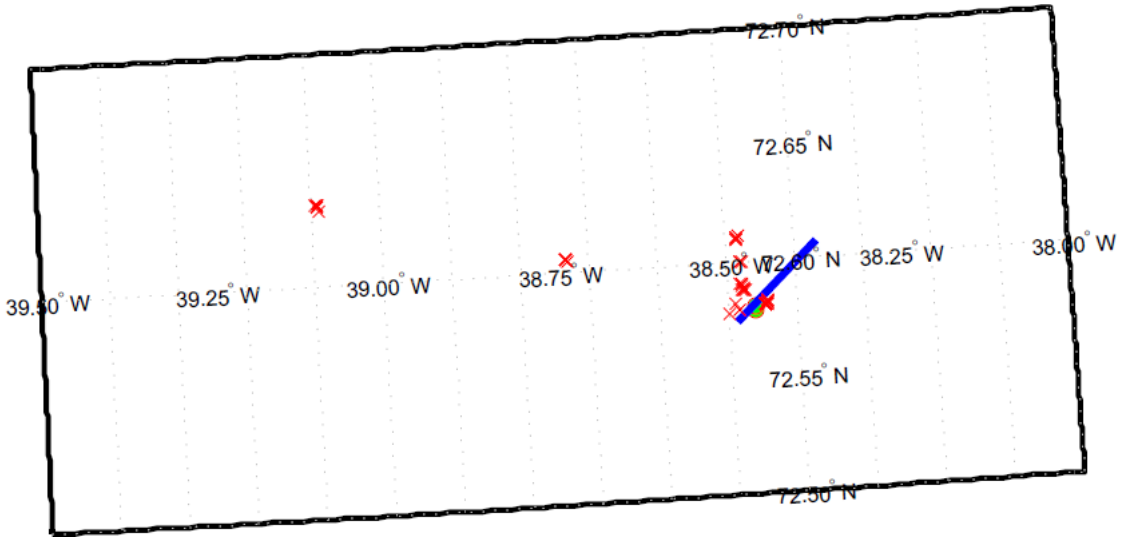

Figure 3.5: The measurement locations visited during RASCALS. The skiway at Summit camp is shown with a blue line, the station location is marked with a green circle next to the southern end of the skiway.

3.2.1 Spectrally resolved and integrated irradiance

We observed the incoming solar radiation using several different instruments. The spectrally resolved irradiance was measured at some points during field days using an ASD FieldSpec 3 spectrometer in irradiance mode with an ASD cosine collector sensor. The spectrally integrated (or shortwave broadband) irradiance was measured by the Kipp & Zonen CM-14 albedometer continuously during the time spent on the field each day. In addition, the FGI FIGIFIGO instrument also recorded the spectrally integrated irradiance, albeit on a narrower waveband than the CM-14.

Table 3.1 shows the times and locations of each spectrally resolved irradiance measured by the ASD FieldSpec during the campaign. The reader may note that the time zone at Summit station is UTC-2 because of daylight saving time. If the observation is marked as "diffuse" in the notes, it means that a cardboard shield was erected to block the direct sunlight from the sensor. The cardboard was large enough and close enough to also block out slightly refracted sunlight that could also be considered as direct Solar radiation. Only the diffuse part of the irradiance is expected to remain in the results. Each sample consists of 30 sweeps of the FieldSpec measurement waveband. After July 13, the weather turned unfavorable with scattered thick clouds which changed the illumination conditions constantly. After July 16 the field observations were all deemed complete and we began packing the equipment for the journey back.

Table 3.1: Observed spectrally resolved irradiances (waveband: 350-2500 nm)

Date, time (UTC)	Latitude (N)	Longitude (E)	Notes (CS=clear sky, sunny)
29.6. 13:59	72.581	-38.448	CS, scattered thin clouds

Table 3.1: Observed spectrally resolved irradiances (waveband: 350-2500 nm)

Date, time (UTC)	Latitude (N)	Longitude (E)	Notes (CS=clear sky, sunny)
30.6. 13:30	72.580	-38.445	CS (Halo visible)
30.6. 18:16	72.593	-38.467	CS (No halo)
1.7. 16:31	72.581	-38.444	CS, clear-sky precip
1.7. 17:29	72.583	-38.442	CS
1.7. 18:06	72.583	-38.442	CS
4.7. 14:48	72.577	-38.445	CS, scattered thin clouds
4.7. 15:05	72.577	-38.445	CS, scattered thin clouds
5.7. 11:21	72.589	-38.445	CS
5.7. 11:24	72.589	-38.445	CS, diffuse
5.7. 11:55	72.589	-38.445	CS
5.7. 12:23	72.589	-38.445	CS
5.7. 16:28	72.588	-38.475	CS
5.7. 16:33	72.588	-38.475	CS, diffuse
5.7. 16:46	72.588	-38.475	CS
5.7. 17:22	72.588	-38.475	CS
5.7. 17:25	72.588	-38.475	CS, diffuse
5.7. 18:40	72.588	-38.475	CS
6.7. 13:09	72.581	-38.446	CS, scatt. thin clouds
6.7. 13:12	72.581	-38.446	CS, diff., scatt. thin clouds
6.7. 16:10	72.581	-38.446	CS, ice crystals
7.7. 12:21	72.610	-38.483	CS
7.7. 13:14	72.611	-38.481	CS
7.7. 17:00	72.611	-38.481	CS
7.7. 17:10	72.611	-38.481	CS, diffuse
8.7. 18:56	72.588	-38.475	CS
8.7. 19:13	72.588	-38.478	CS
9.7. 11:35	72.581	-38.445	Overcast, thin cirrus cl.
9.7. 11:38	72.581	-38.445	Diffuse, overcast, thin cirrus cl.
9.7. 13:28	72.581	-38.445	Overcast, thin cirrus cl.
9.7. 13:30	72.581	-38.445	Diffuse, overcast, thin cirrus cl.
9.7. 15:23	72.581	-38.445	Thick high clouds, Sun disc visible
9.7. 15:26	72.581	-38.445	Diffuse, Thick high clouds, Sun disc visible
9.7. 18:09	72.581	-38.445	Thick high clouds, Sun disc visible
9.7. 18:14	72.581	-38.445	Diffuse, Thick high clouds, Sun disc visible
10.7. 11:46	72.581	-38.445	CS, scattered clouds
10.7. 11:48	72.581	-38.445	Diffuse, CS, scattered clouds
11.7. 14:47	72.581	-38.445	Completely overcast, faint Sun disc
11.7. 14:50	72.581	-38.445	Diffuse, Completely overcast, faint Sun disc
11.7. 14:51	72.581	-38.445	32-min observation series, overcast sky
12.7. 13:35	72.606	-38.735	CS
12.7. 13:43	72.606	-38.735	CS, diffuse
12.7. 17:18	72.634	-39.092	CS
12.7. 17:34	72.633	-39.090	CS
12.7. 19:28	72.634	-39.092	CS
12.7. 22:49	72.581	-38.445	CS
13.7. 11:54	72.581	-38.445	CS
13.7. 11:57	72.581	-38.445	CS, diffuse
13.7. 12:47	72.581	-38.445	CS
13.7. 16:20	72.581	-38.445	CS
13.7. 16:39	72.581	-38.441	CS
13.7. 21:33	72.581	-38.441	CS

Table 3.1: Observed spectrally resolved irradiances (waveband: 350-2500 nm)

Date, time (UTC)	Latitude (N)	Longitude (E)	Notes (CS=clear sky, sunny)
13.7. 21:40	72.581	-38.441	CS, diffuse

3.2.2 Spectral reflectance of snow

In conjunction with the spectral irradiance measurements, we also observed the snow spectral reflectance from nadir using the ASD FieldSpec 3 with a tripod-mounted 8 degree foreoptic. Table 3.2 shows the observations in chronological order. The observations marked with "GQ" in the notes refer to samplings with the best quality; perfectly clear skies ensuring steady illumination coupled with the most careful nadir-leveling of the sensor. These reflectance spectra have the lowest variance across the 30 spectrum sweeps that make up the observation.

Table 3.2: Observed spectrally resolved snow reflectances (waveband: 350-2500 nm)

Date, time (UTC)	Latitude (N)	Longitude (E)	Notes CS=clear sky, sunny / GQ= Good Quality
29.6. 13:59	72.581	-38.448	CS, scattered thin clouds
30.6. 13:30	72.580	-38.445	CS (Halo visible)
30.6. 18:16	72.593	-38.467	CS (No halo)
1.7. 16:10	72.581	-38.444	CS
1.7. 16:16	72.583	-38.442	CS
1.7. 16:23	72.583	-38.442	CS, clear-sky precip
1.7. 17:00	72.583	-38.442	CS
4.7. 15:17	72.577	-38.445	CS, scattered thin clouds
4.7. 15:19	72.577	-38.445	CS, scattered thin clouds
5.7. 11:36	72.589	-38.445	CS
5.7. 11:40	72.589	-38.445	CS
5.7. 11:42	72.589	-38.445	CS
5.7. 18:08	72.589	-38.445	CS
5.7. 18:19	72.588	-38.475	CS
7.7. 12:42	72.610	-38.483	CS, GQ
7.7. 12:57	72.611	-38.481	CS, GQ
7.7. 17:24	72.611	-38.481	CS
8.7. 16:44	72.588	-38.475	CS
8.7. 16:49	72.588	-38.478	CS, GQ
8.7. 19:24	72.588	-38.478	CS
9.7. 11:53	72.581	-38.445	overcast, thin cirrus cl.
9.7. 15:35	72.581	-38.445	Thick high clouds, Sun disc visible
9.7. 18:04	72.581	-38.445	Thick high clouds, Sun disc visible
10.7. 11:42	72.581	-38.445	CS, scattered clouds
11.7. 14:39	72.581	-38.445	Completely overcast, faint Sun disc
12.7. 13:52	72.606	-38.735	CS
12.7. 13:55	72.606	-38.735	CS
12.7. 17:10	72.634	-39.092	CS
12.7. 17:12	72.634	-39.092	CS
12.7. 17:45	72.633	-39.090	CS, GQ
12.7. 19:19	72.634	-39.092	CS
13.7. 12:13	72.581	-38.445	CS
13.7. 12:32	72.581	-38.445	CS
13.7. 12:38	72.581	-38.445	CS, GQ
13.7. 16:48	72.581	-38.441	CS

Table 3.2: Observed spectrally resolved snow reflectances (waveband: 350-2500 nm)

Date, time (UTC)	Latitude (N)	Longitude (E)	Notes CS=clear sky, sunny / GQ= Good Quality
13.7. 21:48	72.581	-38.441	CS

In figure 3.6 we show an example of the snow spectra measured during RASCALS. The graph is the mean of the 30 spectra recorded by the ASD FieldSpec at that location. The reflectance is measured at nadir, i.e. the foreoptic is mounted on a tripod and leveled to look directly downward at the snowpack. Most of the measured reflectance spectra show very low variances across the 30 sample sweeps. The exceptions are the cases in which there are scattered or thicker clouds near the Sun. This is expected, since the irradiance spectra is modified even when the clouds are not in the direct line-of-sight between the measurement location and the Sun.

In all cases, the reflectance observation is made in the same way. First, the spectrometer aligned so that its shadow points directly away from the observation area. Next, the spectrometer is calibrated for dark current using a LabSphere reference spectralon as a target. Then, the same spectralon is used as a white reference for the reflectance measurement. The reference spectralon sits on the snow surface in a protective casing. We have found that mounting the spectralon close to the foreoptic does have an effect on the observed radiance. To prevent this, we place the spectralon at snow surface level to ensure equal viewing geometry for both calibration and observation. In some cases we recorded the spectralon reflectance for 30 ASD waveband sweeps to verify the stability of the illumination conditions. This auxiliary data is also available upon request. After the calibration, we generally move the tripod slightly (10-15 cm laterally), check leveling again, and then measure the snow reflectance.

During the campaign we also found that the snow reflectance in the UV range (350-500 nm) is highly sensitive to the amount of clear sky that is "visible" to the observation area. This means that if the spectrometer operator happens to stand too close to the observation area during the measurement, or move around, the UV reflectance measurement will be disturbed. As this was found out during the first week of operations at Summit, we advise users to be very careful when using the nadir snow reflectances from the time period 29.6. - 4.7.

3.2.3 Broadband albedo of snow

The primary variable of interest for the campaign, snow broadband albedo, was directly measured with the Kipp & Zonen CM-14 Albedometer. Measurements mainly took place coincidentally with the other radiative and physical measurements. The albedometer was not used continuously because the observation site changed daily and thus the albedometer needed to be moved too. Also, the albedometer was not fitted with heating/ventilation gear. Experiments showed that frost formed on both upper and lower collector domes of the albedometer during night-time, making the data unreliable.

Figure 3.7 shows a day during the campaign where the albedometer was stationary from morning till night. While not visible in the this figure, the effect of frost formation on the albedometer domes was observed during the evenings of some observation days. The frost will particularly inhibit the irradiance sensor from seeing the sky, thus dropping the observed incoming radiation level. As frost tends to form strongest on upward-facing surfaces that "see" the cold sky, the reflected radiation dome is less affected. As a result, the observed albedo is strongly biased toward higher values. The albedo data has been screened to remove all frost-contaminated observation periods.

In contrast, there also are disturbances in irradiance and reflected irradiance that relate to a natural phenomenon - cloudiness. Clouds passing over the Sun reduce incoming radiation intensity at ground level relatively more than the reflected radiation, thus causing an increase in albedo in accordance with theory. Misinterpretation between clouds and frost formation is highly unlikely, as typically frost cannot form on the albedometer domes during daytime because of the high Solar input (max at $\approx 800\ W/m^2$).

There were several interesting albedo phenomena observed during the campaign. During the evenings and nights when the Sun drew closer to the horizon, the snowpack surface underwent

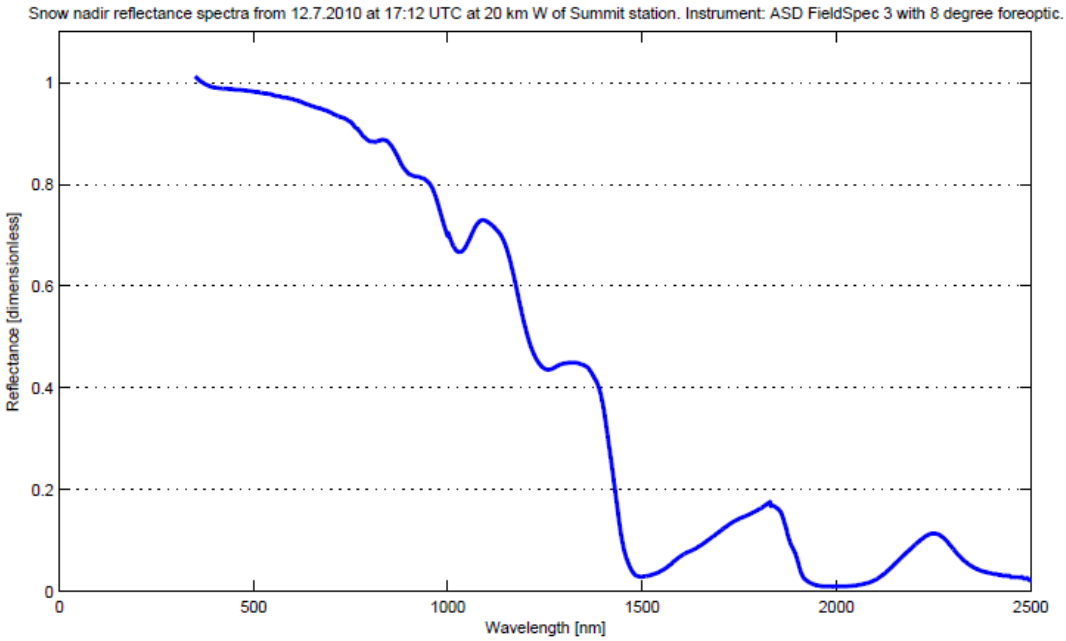

Figure 3.6: A snow reflectance spectrum observed at 12 July 17:12 UTC. The sample was a typical rime-covered fluffy snowpack composed of dendritic crystals.

changes on several occasions. Apparently, the frost forming on the snowpack surface created spherical growths of ice crystals up to centimeter-scale heights (surface hoar). Combined with low Sun elevation, this phenomenon created small-scale geometric shadowing on the snowpack surface which also showed in the observed albedo as a decrease. The study of this effect is still ongoing, but visual observation and photographs seem to confirm the presence of small-scale shadows on the snowpack surface around 23 UTC on one of the days that the albedo data showed a decrease toward night-time.

Overall, the snow albedo was stable over the campaign period and showed little dependency on location. This is in accordance with existing theory. The top of the Greenland Ice Sheet is at over 3000 a.s.l., and has no real topography. We observed small-scale snow drifts and substantial changes in the hardness of the surface layer. Therefore we can say that physical differences exist in the snowpack even though their effect on the radiative properties of snow appear minor.

Table 3.3 shows the time periods and locations covered by the albedometer measurements. The data listed here has been quality-controlled for frost formation. The QA approach was to fit a RTM-simulated clear-sky irradiance curve to the actual measurements and visually confirm if the irradiances appear physical. In principle, during daylight hours the albedometer is stable and frost effects cannot affect the measurements because of constant operator supervision and the heating effect of solar radiation. The comparison to the RTM simulation during night-time reveals the periods when frost formation on the domes begins to distort the measurement. The data is then removed until the period of the next dome cleaning event.

The CM 14 calibration was checked during spring 2011 against a reference pyranometer at FMI. The upper pyranometer showed no discernible bias, but the lower pyranometer showed a -15.4 W/m^2 bias. The data has been corrected for this bias.

Another issue in the albedometer data calibration is the correction for the instrument set-up geometry. The tripod on which the instrument is mounted will block some of the reflected radiation from reaching the detector dome, thus creating a negative bias in the albedo. The effect is strongest when observing snow, as the dark carbon fiber material of the tripod contrasts very strongly with bright snow. To correct for this effect, we measured the solid angle of the lower hemisphere that is blocked by the tripod (relative to total area), and then applied the FIGIFIGO HDRF data to

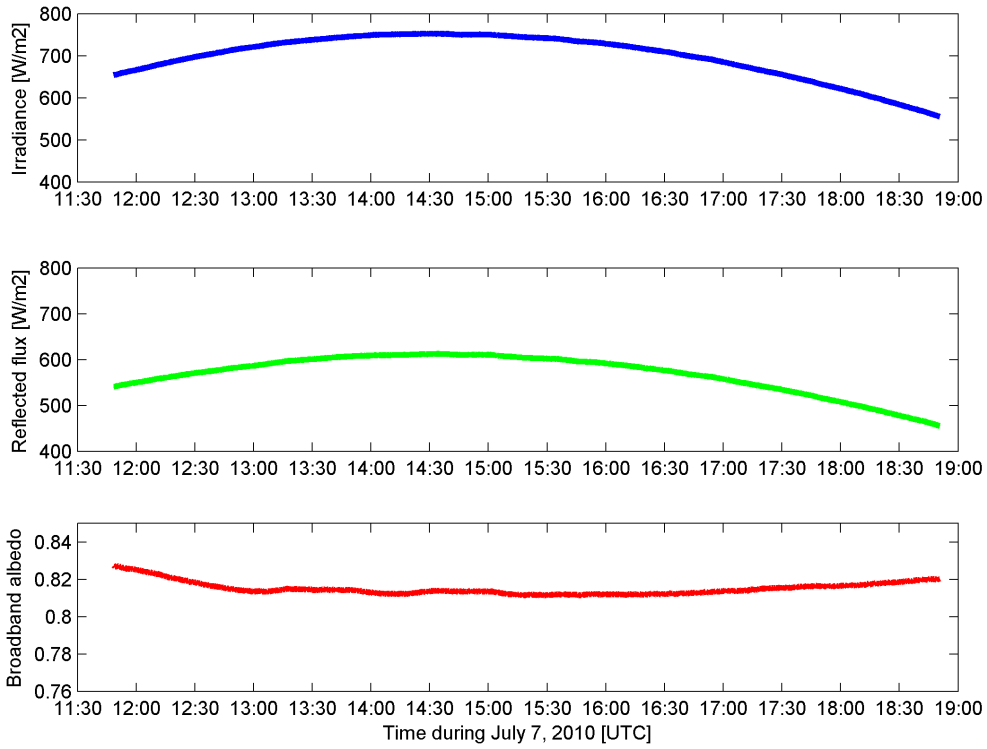

Figure 3.7: An example of the observed incoming irradiance (top), reflected irradiance (middle) and snow broadband albedo (bottom) from RASCALS, July 7, 2010. The observed waveband is 350-2800 nm.

Table 3.3: Periods of collected and quality-controlled broadband albedo data with the Kipp & Zonen CM-14

Date (in 2010)	Measurement start (UTC)	Measurement stop (UTC)	Comments CS=clear sky, sunny
29.06.	12:07	16:44	CS
30.06.	11:35	13:19	CS
30.06.	16:19	18:11	CS
01.07.	11:20	23:59	CS from 14UTC
02.07.	00:00	11:27	Cloudy
03.07.	11:03	23:59	Cloudy
04.07.	00:00	00:32	CS
04.07.	14:18	23:59	CS
05.07.	00:00	01:32	CS
05.07.	11:05	12:29	CS
05.07.	17:20	20:14	CS
06.07.	11:06	23:00	CS with scatt. clouds
07.07.	11:48	18:50	CS
09.07.	11:11	23:59	Cloudy
10.07.	00:00	23:59	CS until 10UTC, then cloudy
11.07.	02:16	23:59	Cloudy
12.07.	00:00	05:14	CS
12.07.	12:52	14:50	CS
12.07.	16:29	19:38	CS
12.07.	19:38	23:59	CS
13.07.	00:00	05:28	CS
13.07.	11:39	23:59	CS
15.07.	11:43	23:59	Cloudy
16.07.	00:00	15:22	Cloudy
16.07.	15:22	17:46	Cloudy
17.07.	11:36	23:59	Cloudy
18.07.	00:00	23:59	CS until 08UTC, then cloudy
19.07.	00:00	12:58	CS until 11UTC, then cloudy

estimate the amount of radiation that is thus blocked. The correction has a modest dependency on solar position because of the strong forward-scattering characteristic of snow. A typical correction is +6.5% to +7% (relative) in the reflected radiation. The correction factor is calculated separately for all days for which appropriate FIGIFIGO data is available for analysis, and the most common correction of +6.6% is used otherwise.

Figure 3.8 shows the albedometer in measurement configuration near Summit station. As mentioned in the previous paragraph, the effect of the tripod chassis on the observed albedo is known and can be compensated for. The data logger unit is not shown in the picture. A known issue with long-duration measurements is that the albedometer has no capability to track the Sun. Thus, when the albedometer is set up in the morning facing the Sun (thus its shadow "points" away from it), by late evening the instrument's shadow will have moved underneath it. Since the albedometer gathers its reflected signal from an area of over 700 m^2, the location of the shadow should have little effect on the integrated reflected irradiance. However, manufacturer specifications suggest always pointing the instrument arm toward Sun, so it must be taken into account that there may be some directional effects in the observed irradiance and reflected irradiance.

3.2.4 Hemispherical-Directional reflectance (HDRF) and bidirectional reflectance (BRF) of snow

The FGI FIGIFIGO instrument is capable of measuring the Hemispherical-Directional reflectance (HDRF) and bidirectional reflectance (BRF) of snow over a short time period. The measurement

Figure 3.8: The Kipp & Zonen CM-14 Albedometer in measurement configuration.

procedure was as follows. After selecting a suitable measurement area FIGIFIGO was assembled. A white reference spectrum was obtained from a 25x25 cm^2, 99% reflective Spectalon (Labsphere inc.). The diffuse illumination from surroundings was measured by blocking the direct sun direction and measuring a spectrum from both Spectralon and the snow target. The snow surface sample of 20-50 cm in diameter was measured with zenith angles of $\pm 80°$from nadir and at azimuth angles of 0°, 10°, 20°, 40°, 60°, 80°, 90°, 120°, and 160°from principal plane. As the instrument was manually rotated for azimuth angle and the actual angle was measured, these figures may vary. The zenith angle resolution was 2-5°. The white reference and diffuse spectra were obtained periodically during and after the measurement to take into account the changing illumination conditions, and the pyranometer was constantly recording the irradiance. Small changes were corrected in post processing using the pyranometer data, and measurement was aborted if illumination changed considerably.

Close to 50 observations of snow directional reflectance signature were carried out during RASCALS. The measurement times and locations are listed in Table 3.4. The measurements covered most of the possible SZAs for the time of year at Summit camp. The distribution of FIGIFIGO measurements as a function of SZA is illustrated in Figure 3.9.

During postprocessing, any data affected by e.g. foreoptic boom shadows or other disturbances are first removed. The observed angular reflectances are then interpolated into a full hemispherical reflectance distribution. If desired, the data may be outputted as either a HDRF or a BRF as the diffuse illumination correction is either off or on, respectively. The final data may be visualized, an example of the ready HDRF profile is shown in Figure 3.10.

3.2.5 Accuracy assessment of the radiative measurements

Inaccuracies in the broadband albedo measurements have the following main sources: First, frost or other obstructions on the domes limit the radiation reaching the detector(s). Experiments showed that frost formed on both upper and lower collector domes of the albedometer during some RASCALS overnight measurements. The erroneous data was purged by visually comparing all irradiance observations to clear-sky RTM simulations and removing all suspect data.

Second, since the CM 14 we use is not ventilated, the zero offset resulting from a temperature difference between the detector and chassis cold junction will apply. Kipp & Zonen gives an upper value for this offset as 12 W/m^2 with 200 W/m^2 thermal radiation with no ventilation. Considering that as a baseline and assuming that the offset does not increase linearly with increasing thermal radiation, we may safely assume an upper limit of 3-4% relative error in irradiance (and therefore

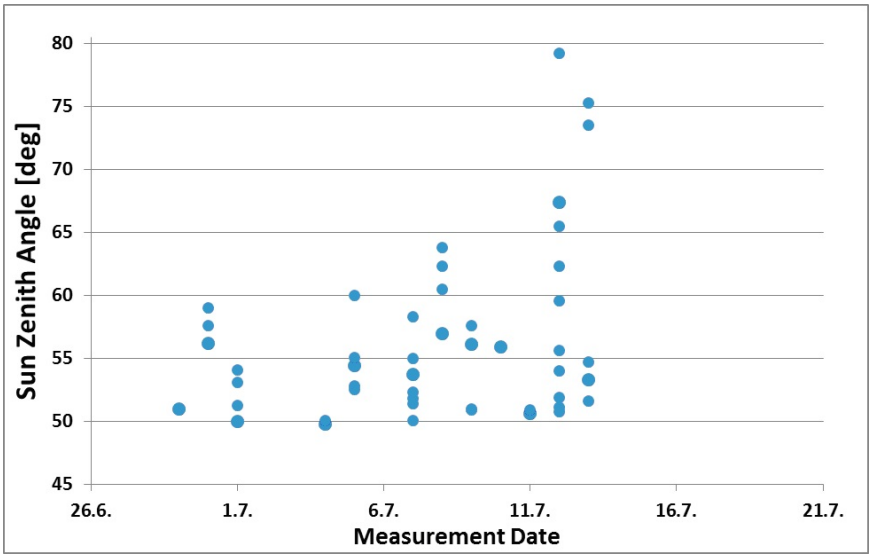

Figure 3.9: The distribution of FIGIFIGO measurements as a function of Sun Zenith Angle (SZA) during RASCALS.

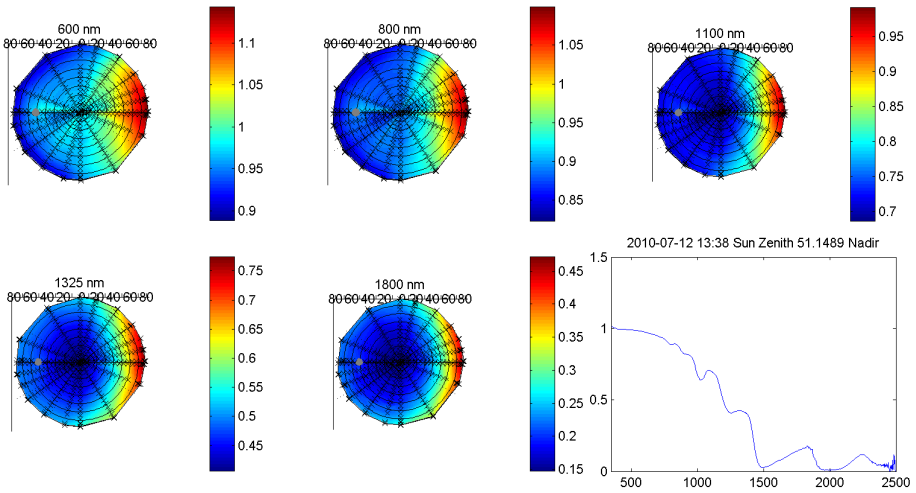

Figure 3.10: An example of the FIGIFIGO HDRF data from July 12, 13:38 UTC.

Table 3.4: FIGIFIGO observations of snow HDRF/BRF during RASCALS

Measurement Date and ID	Time (UTC)	Latitude (N)	Longitude (W)	Comments
2010-06-29-Snow1	13:48	72d34.861m	38d26.845m	
2010-06-30-Snow1	18:43	72d35.594m	38d28.063m	
2010-06-30-Snow2	19:03	72d35.600m	38d28.058m	
2010-06-30-Snow3	19:28	72d35.599m	38d28.053m	Principle planes only
2010-07-01-Snow1	16:12	72d34.407m	38d25.922m	
2010-07-01-Snow2	17:01	72d34.906m	38d26.651m	
2010-07-01-Snow3	17:35	72d34.931m	38d26.575m	
2010-07-01-Snow4	18:05	72d34.958m	38d26.572m	
2010-07-04-Snow1	14:35	72d34.604m	38d22.383m	
2010-07-04-Snow2	15:05	72d34.889m	38d26.773m	
2010-07-05-Snow1	11:37	72d34.869m	38d26.719m	
2010-07-05-Snow2	12:22	72d34.867m	38d26.691m	
2010-07-05-Snow3	16:05	72d34.870m	38d26.710m	
2010-07-05-Snow4	17:13	72d35.315m	38d28.532m	
2010-07-05-Snow5	17:51	72d35.315m	38d28.532m	Polarizations 0,90,45,135
2010-07-07-Snow1	11:57	72d38.615m	38d31.943m	
2010-07-07-Snow2	12:32	72d36.590m	38d28.993m	
2010-07-07-Snow3	13:01	72d36.600m	38d28.997m	
2010-07-07-Snow4	15:33	72d36.604m	38d28.945m	
2010-07-07-Snow5	16:00	72d36.596m	38d28.960m	
2010-07-07-Snow6	16:53	72d36.605m	38d28.953m	Polarizations 0,90,45,135
2010-07-07-Snow7	17:59	72d36.615m	38d28.969m	Principle planes only
2010-07-08-Snow1	17:20	72d35.281m	38d28.648m	Double angular density
2010-07-08-Snow2	18:37	72d35.267m	38d28.533m	
2010-07-08-Snow3	19:02	72d35.265m	38d28.536m	
2010-07-08-Snow4	19:28	72d35.252m	38d28.519m	Some clouds
2010-07-09-Snow1a	11:19	72d34.880m	38d26.720m	Same measurement spot
2010-07-09-Snow1b	13:16	72d34.880m	38d26.717m	Same measurement spot
2010-07-09-Snow1c	15:18	72d34.885m	38d26.701m	Same measurement spot
2010-07-09-Snow1d	17:53	72d34.656m	38d29.900m	Same measurement spot
2010-07-10-Snow1e	11:28	72d34.878m	38d26.727m	Same measurement spot
2010-07-11-S1Diff	14:42	72d34.878m	38d26.718m	Overcast conditions
2010-07-11-S2Diff	15:11	72d34.881m	38d26.719m	Overcast conditions
2010-07-12-Snow1	08:46	72d34.882m	38d26.707m	
2010-07-12-Snow2	09:13	72d34.883m	38d26.693m	
2010-07-12-Snow3	13:07	72d36.348m	38d44.052m	
2010-07-12-Snow4	13:38	72d36.301m	38d43.806m	
2010-07-12-Snow5	14:08	72d36.349m	38d44.027m	
2010-07-12-Snow6	16:40	72d38.099m	39d05.518m	
2010-07-12-Snow7	17:12	72d38.094m	39d05.534m	
2010-07-12-Snow8	18:16	72d38.102m	39d05.548m	
2010-07-12-Snow9	18:55	72d38.102m	39d05.577m	
2010-07-12-Snow10	22:34	72d34.953m	38d29.336m	Polarizations 0,90,45,135
2010-07-13-Snow3	16:32	72d34.896m	38d25.696m	Polarizations 0,90,45,135
2010-07-13-Snow4	21:23	72d34.883m	38d26.653m	
2010-07-13-Snow5	21:51	72d34.887m	38d26.657m	

in albedo). Other instrument-related inaccuracies are smaller and may partially cancel each other. The first 20 minutes of each day's CM 14 data have been excluded from analysis to ensure a stable operating temperature.

Thirdly, instrument leveling errors may have a substantial impact on the data when the Sun is low. Our data is mainly from periods when the Sun Zenith Angle (SZA) is below 70 degrees. The typical leveling error effect for these periods has been found to be no more than 2-3 W/m^2. We do not correct for tilt errors as their effect in our data is very difficult to detect.

Finally, the tripod on which the albedometer was fitted will block some of the reflected radiation intended to reach the downward-looking pyranometer (Figure 3.8). We modeled the tripod obstruction effect by 1) hemispherical photography to calculate the obstruction magnitude in the pyranometer field-of-view, 2) assumption of an ideal cosine response in the pyranometer and 10% reflectance for the tripod itself, and 3) by applying directional reflectance measurements of snow from RASCALS to account for the surface anisotropy. The obstruction magnitude depends also on solar azimuth during clear-sky conditions. Calculations showed that between 6.6% and 9% of reflected radiation is blocked by the tripod, depending on snow anisotropy and solar direction (azimuth) relative to tripod. Footprints and other snow surface disturbances caused by the operator setting up the instrument may also affect the snow albedo. We estimate their effect is very small for the RASCALS data, as the hard surface snow on the GIS resists footprints quite well.

Overall, the broadband albedo and irradiance are estimated to have an uncertainty of 3-6% after the corrections. For data from periods when SZA was below 70 degrees, we assume an uncertainty of 3%, and 6% otherwise.

The uncertainty of the ASD snow reflectance and irradiance measurements are assumed to be comparable to other published estimates of uncertainty for ASD measurements, i.e. 5% (relative) of reflectance/irradiance [3]. The same error estimate applies also for the FIGIFIGO measurements.

3.3 Observed physical characteristics of snow

Table 3.5 shows the dates, locations and number of samples taken for each manually measured snow physical parameter. These parameters are described in the following sections. The grouping has been done so that measurements made in the close vicinity of the shown coordinates are reported on one line. A snow pit under study is shown in Figure 3.11.

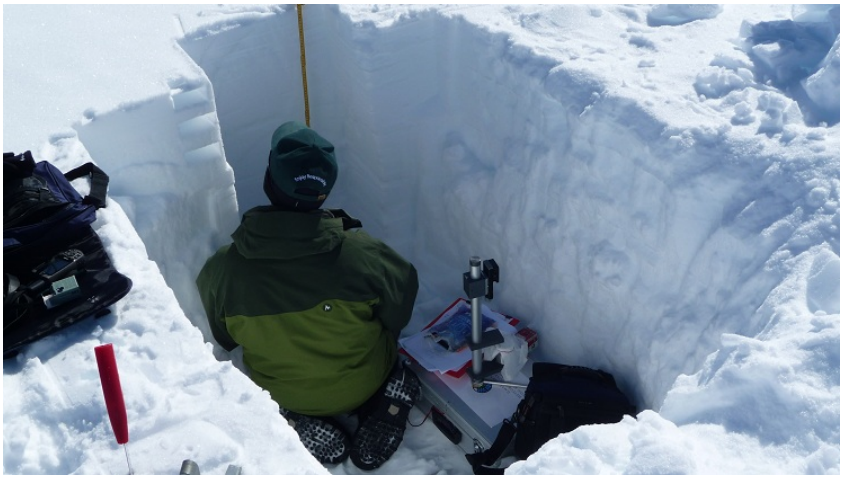

Figure 3.11: A snow pit under study at Summit on July 1, 2010.

3.3.1 Grain size

During the field campaign, no grain size estimates were directly made. From each snow pit, macro photographs (magnification of 2.1 was used) of snow grains were taken from the surface and from

each distinct layer down to 1 meter depth. Also a scale photograph was taken with the same setup before and after each profile. Altogether 758 grain samples were photographed.

3.3.2 Snow temperature profiles

Snow temperature was measured using three different instruments, shown in table 2.1. In snow pits, two digital thermometers were used to record the temperature profile every 2 cm at depths between surface and 10 cm, and every 5 cm from 10 cm downwards. The lowest depth varied between 60 cm and 200 cm in normal snow pits. An illustration of the temperature profiles from July 1 - July 7, 2010 is shown in Figure 3.12.

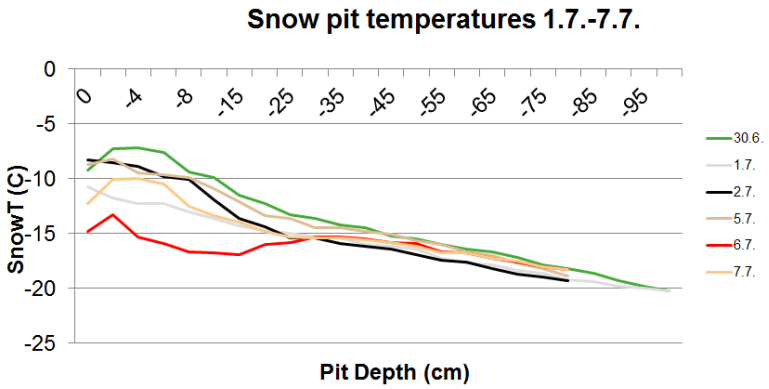

Figure 3.12: Snow temperature profiles from snow pit measurements between July 1 - July 7, 2010.

Two timeseries were made with similar depth increments. The first time series consists of six profiles, the second of five profiles. Time series were made on concecutive days, and each spanning a time frame of 10 hour.

The automatic time series were made using Fluke 1524 + 5618B probe. This instrument was located close to the albedometer to record the temperature change close to the snow surface during the measurement.

Third snow temperature dataset comes from the T-logger, which recorded altogether 15 profiles. The logger was placed close to the albedometer.

3.3.3 Snow density profiles

Snow density profiles were taken from every 5 cm thick layer from 10 cm below the surface down to at most 200 cm depth. In addition, the top layers were measured using a 2 cm thick sampler from 2 cm and 6 cm depths. Altogether 14 of such profiles were measured. The density profiles measured between July 1 - July 7, 2010, are illustrated in Figure 3.13.

3.3.4 Snow dielectric profiles

Snow dielectric parameters were measured using Toikka snow fork. The profiles were done using the same sampling as the density profiles. Altogether 9 profiles were measured.

3.3.5 Snow surface roughness

Snow surface rougness data were collected at albedometer, goniometer and spectrometer sites, and also at snow pit locations. Two timeseries were collected to see the diurnal variation. After quality control (removal of images with bad focus or non-ideal insertion of the imaging plate), 370 roughness profiles were left for analysis.

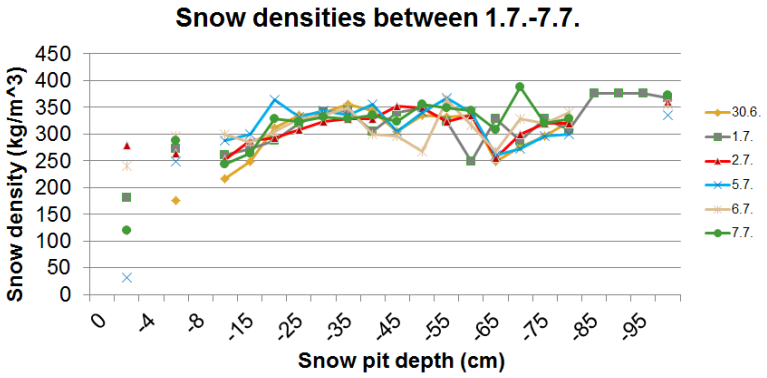

Figure 3.13: Snow density profiles from snow pit measurements between July 1 - July 7, 2010.

3.3.6 Accuracy assessment of the physical measurements

The snow grain macro photographs can be referenced to a spatial accuracy of approximately 0.05 mm. With a suitable software, the 2-dimensional grain measures can be calculated. Also, the photos can be used for visual estimation of the dimensions, or used as a reference to identify the grain type.

Uncertainties of temperature profiles come from depth accuracy, ie. how accuratedly the thermometer was inserted to a certain depth, and from the measurement accuracy. The inaccuracies in depth are around ± 1 cm. The temperatures in the lower levels are accurate within ± 0.2 degrees (for profile measurements). For temperature readings near the surface, the accuracy is lower due to differences in shading used for blocking the direct sun-light. For the Fluke 1524 this illumination is the main source of error, as the sensor it self is accurate to within $\pm 0.066\ ^{\circ}C$. The T-log thermistors and the infrared thermometer have an accuracy of $\pm 0.5\ ^{\circ}C$. For thermistors, the sun-light can cause a significant and variable bias, but the IR thermometer is not affected by sun's heating. For IR thermometer, the output is brightness temperature. To convert this to physical temperature, the actual emissivity of snow needs to be known.

Snow density volumetric measurements can be assumed to be accurate to $\pm 5\%$, the main error source being the used scale which has a resolution of 2 grams. Every sample was inspected visually to have filled the whole sampler before weighting.

The measurement method used in the snow fork for dielectric constant is reported to have an accuracy of $\pm 1.5\%$ [6]. The repeatability of the measurements differ depending on the snow type, but for the dense, hard snow of Greenland the measurements can be assumed to be highly repeatable.

There are two main aspects that control the quality of snow surface roughness determination. The greater of these is the insertion of the reference background to snow so that the snow surface is disturbed as little as possible. If the snow – air interface is disturbed, the data needs to be rejected. The other issue is the the imaging geometry. Although all the images are rectified to same image coordinate system, the angle of imaging relative to background affects how the surface is observed. Also the variation of camera zoom and illumination conditions cause variation in the spatial resolution and achievable accuracy.

Table 3.5: Measurements of snow physical parameters. Number of profiles and number of samples (in parentheses). GS: grain size macro photographs, T: temperature, ρ: snow density, ϵ: dielectric constant, SSR: snow surface roughness, NIR: near-infrared photographs.

Date	Latitude	Longitude	GS (#)	T (#)	ρ (#)	ϵ (#)	SSR (#)	NIR (#)
29.6.	72°34.860'	-38°26.868'	-	2 (16)	1 (4)	1 (4)	3 (9)	-
30.6.	72°35.608'	-38°28.041'	1 (12)	2 (34)	1 (20)	-	3 (9)	-
1.7.	72°34.878'	-38°26.793'	5 (98)	1 (25)	1 (21)	1 (21)	9 (26)	1 (4)
2.7.	72°35.987'	-38°28.694'	1 (42)	1 (25)	1 (21)	1 (21)	3 (9)	1 (3)
4.7.	72°34.864'	-38°26.711'	1 (11)	1 (8)	-	-	6 (18)	-
5.7.	72°35.297'	-38°28.552'	2 (48)	2 (33)	1 (21)	1 (21)	18 (53)	1 (3)
6.7.	72°34.865'	-38°28.746'	1 (34)	1 (25)	1 (21)	1 (21)	3 (9)	1 (4)
7.7.	72°36.607'	-38°28.990'	2 (99)	2 (38)	1 (21)	1 (21)	38 (86)	1 (4)
8.7.	72°35.279'	-38°28.662'	1 (70)	1 (16)	1 (14)	1 (13)	4 (36)	-
9.7.	72°34.875'	-38°26.733'	6 (112)	6 (66)	-	-	18 (18)	-
10.7.	72°34.875'	-38°26.733'	5 (94)	5 (55)	-	-	13 (13)	-
12.7.	72°36.356'	-38°44.077'	1 (35)	1 (25)	1 (21)	1 (21)	12 (36)	-
12.7.	72°38.088'	-39°05.519'	1 (49)	1 (25)	1 (22)	1 (21)	12 (36)	1 (3)
12.7.	72°34.874'	-38°26.732'	1 (14)	1 (11)	-	-	3 (4)	-
13.7.	72°38.847'	-38°26.746'	-	1 (40)	-	-	3 (27)	-
15.7.	72°34.876'	-38°26.688'	1 (25)	3 (74)	2 (39)	1 (31)	39 (39)	1 (15)
16.7.	72°37.600'	-38°29.901'	1 (15)	2 (48)	-	1 (20)	3 (8)	-
19.7.	72°34.875'	-38°26.650'	-	1 (13)	-	-	-	-
total			30 (758)	34 (577)	12 (225)	11 (215)	190 (454)	7 (36)

Chapter 4

Discussion

This report introduces the RASCALS campaign, its goals, methods, and collected data. The campaign was designed around the idea of concurrent measurements of arctic perennial snow albedo, its physical drivers, and its spectral reflectance signature. The data was collected during three weeks at the Greenland Geophysical Observatory at Summit camp on the top of the Greenland Ice Sheet during June-July 2010.

Overall, the measured variables are in line with previous studies, where such exist. The directional reflectance dataset collected during RASCALS is to our knowledge the largest ever recorded on the Greenland Ice Sheet. Also, concurrent snow grain and albedo observations from the GIS have been rare previously. We did not possess the capability to perform snow impurity measurements; fortunately several other authors ([7]) have made such observations at Summit camp, thus giving a baseline for estimating BC content at the site. The station staff also provided us with atmospheric profile and weather station data, which is thankfully acknowledged.

The campaign was successful as a large dataset of snow albedo, snow physical characteristics, and snow directional reflectances was collected. Much of the data is from clear-sky conditions owing to a spell of fine weather at Summit during the campaign. Thus, its value to validation and development of optical satellite remote sensing of snow should be considerable. The data has been subjected to quality assurance procedures by the instrument operators. After initial scientific publications, the data is intended to be released for the scientific community for further exploitation.

Bibliography

[1] David A. Robinson, Kenneth F. Dewey, and Richard R. Heim, Jr. Global snow cover monitoring: An update. *Bulletin of the American Meteorological Society*, 74(9):1689–1696, 1993.

[2] J.I. Peltoniemi, S. Kaasalainen, J. Naranen, L. Matikainen, and J. Piironen. Measurement of directional and spectral signatures of light reflectance by snow. *IEEE Transactions on Geoscience and Remote Sensing*, 43(10):2294–2304, 2005.

[3] Jouni I. Peltoniemi, Sanna Kaasalainen, Jyri Näränen, Miina Rautiainen, Pauline Stenberg, Heikki Smolander, Sampo Smolander, and Pekka Voipio. BRDF measurement of understory vegetation in pine forests: dwarf shrubs, lichen, and moss. *Remote Sensing of Environment*, pages 343–354, 2005.

[4] P. Lahtinen. Brief communication "snow profile associated measurements (spam) - a new instrument for quick snow profile measurements". *The Cryosphere Discussions*, 5(3):1737–1748, 2011.

[5] K Steffen, J.E. Box, and W. Abdalati. Greenland climate network: Gc-net. *CRREL 96-27 Special Report on Glaciers, Ice Sheets and Volcanoes, tribute to M. Meier*, pages 98–103, 1996.

[6] A. Sihvola and M. Tiuri. Snow fork for field determination of the density and wetness profiles of a snow pack. *IEEE Trans. Geosci. Remote Sens.*, 24(5):717–721, 1986.

[7] S.J. Doherty, S.G. Warren, T.C. Grenfell, A.D. Clarke, and R.E. Brandt. Light-absorbing impurities in arctic snow. *Atmospheric Chemistry and Physics*, 10:11647–11680, 2010.

List of Figures

List of Tables

RAPORTTEJA - RAPPORTER - REPORTS

1986:

1. Savolainen, Anna Liisa et al., 1986. Radioaktiivisten aineiden kulkeutuminen Tshernobylin ydinvoimalaonnettomuuden aikana. Väliaikainen raportti. 39 s.

2. Savolainen, Anna Liisa et al., 1986. Dispersion of radioactive release following the Chernobyl nuclear power plant accident. Interim report. 44 p.

3. Ahti, Kari, 1986. Rakennussääpalvelukokeilu 1985-1986. Väliraportti Helsingin ympäristön talvikokeilusta 18.11.-13.3.1986. 26 s.

4. Korhonen, Ossi, 1986. Pintatuulen vertailumittauksia lentoasemilla. 38 s.

1987: 1. Karppinen, Ari et al., 1987. Description and application of a system for calculating radiation doses due to long range transport of radioactive releases. 50 p.

2. Venäläinen, Ari, 1987. Ilmastohavaintoihin perustuva arvio jyrsinturpeen tuotantoedellytyksistä Suomessa. 35 s.

3. Kukkonen, Jaakko ja Savolainen, Anna Liisa, 1987. Myrkyllisten kaasujen päästöt ja leviäminen onnettomuustilanteissa. 172 s.

4. Nordlund, Göran ja Rantakrans, Erkki, 1987. Matemaattisfysikaalisten ilmanlaadun arviointimallien luotettavuus. 29 s.

5. Ahti, Kari, 1987. Rakennussäätutkimuksen loppuraportti. 45 s.

6. Hakola, Hannele et al., 1987. Otsonin vaihteluista Suomessa yhden vuoden havaintoaineiston valossa. 64 s.

7. Tammelin, Bengt ja Erkiö, Eero, 1987. Energialaskennan säätiedot - suomalainen testivuosi. 108 s.

1988:

1. Eerola, Kalle, 1988. Havaintojen merkityksestä numeerisessa säänennustuksessa. 36 s.

2. Fredrikson, Liisa, 1988. Tunturisääprojekti 1986-1987. Loppuraportti. 31 s.

3. Salmi, Timo and Joffre, Sylvain, 1988. Airborne pollutant measurements over the Baltic Sea: meteorological interpretation. 55 p.

4. Hongisto, Marke, Wallin, Markku ja Kaila, Juhani, 1988. Rikkipäästöjen vähentämistoimenpiteiden taloudellisesti tehokas valinta. 80 s.

5. Elomaa, Esko et al., 1988. Ilmatieteen laitoksen automaattisten merisääasemien käyttövarmuuden parantaminen. 55 s.

6. Venäläinen, Ari ja Nordlund, Anneli, 1988. Kasvukauden ilmastotiedotteen sisältö ja käyttö. 63 s.

7. Nieminen, Rauno, 1988. Numeeristen paine- ja ja korkeuskenttäennusteiden objektiivinen verifiointisysteemi sekä sen antamia tuloksia vuosilta 1985 ja 1986. 35 s.

1989:

1. Ilvessalo, Pekko, 1989. Yksittäisestä piipusta ilmaan päästevien epäpuhtauksien suurimpien tuntipitoisuuksien arviointimenetelmä. 21 s.

1992:

1. Mhita, M.S. and Venäläinen, Ari, 1991. The variability of rainfall in Tanzania. 32 p.

2. Anttila, Pia (toim.), 1992. Rikki- ja typpilaskeuman kehitys Suomessa 1980-1990. 28 s.

1993:

1. Hongisto, Marke ja Valtanen Kalevi, 1993. Rikin ja typen yhdisteiden kaukokulkeutumismallin kehittäminen HIRLAM-sääennustemallin yhteyteen. 49 s.

2. Karlsson, Vuokko, 1993. Kansalliset rikkidioksidin analyysivertailut 1979 - 1991. 27 s.

1994:

1. Komulainen, Marja-Leena, 1995. Myrsky Itämerellä 28.9.1994. Säätilan kehitys Pohjois-Itämerellä M/S Estonian onnettomuusyönä. 42 s.

2. Komulainen, Marja-Leena, 1995. The Baltic Sea Storm on 28.9.1994. An investigation into the weather situation which developed in the northern Baltic at the time of the accident to m/s Estonia. 42 p.

1995:

1. Aurela, Mika, 1995. Mikrometeorologiset vuomittausmenetelmät - sovelluksena otsonin mittaaminen suoralla menetelmällä. 88 s.

2. Valkonen, Esko, Mäkelä, Kari ja Rantakrans, Erkki, 1995. Liikenteen päästöjen leviäminen katukuilussa - AIG-mallin soveltuvuus maamme oloihin. 25 s.

3. Virkkula, Aki, Lättilä, Heikki ja Koskinen, Timo, 1995. Otsonin maanpintapitoisuuden mittaaminen UV-säteilyn absorbtiolla: DOAS-menetelmän vertailu suljettua näytteenottotilaa käyttävään menetelmään. 29 s.

4. Bremer, Pia, Ilvessalo, Pekko, Pohjola, Veijo, Saari, Helena ja Valtanen, Kalevi, 1995. Ilmanlaatuennusteiden ja -indeksin kehittäminen Helsingin Käpylässä suoritettujen mittausten perusteella. 81 s.

1996:

1. Saari, Helena, Salmi, Timo ja Kartastenpää, Raimo, 1996. Taajamien ilmanlaatu suhteessa uusiin ohjearvoihin. 98 s.

1997:

1. Solantie, Reijo, 1997. Keväthallojen alueellisista piirteistä ja vähän talvipakkastenkin. 28 s.

1998:

1. Paatero, Jussi, Hatakka, Juha and Viisanen, Yrjö, 1998. Concurrent measurements of airborne radon-222, lead-210 and beryllium-7 at the Pallas-Sodankylä GAW station, Northern Finland. 26 p.

2. Venäläinen, Ari ja Helminen, Jaakko, 1998. Maanteiden talvikunnossapidon sääindeksi. 47 s.

3. Kallio, Esa, Koskinen, Hannu ja Mälkki, Anssi, 1998. VII Suomen avaruustutkijoiden COSPAR-kokous, Tiivistelmät. 40 s.

4. Koskinen, H. and Pulkkinen, T., 1998. State of the art of space weather modelling and proposed ESA strategy. 66 p.

5. Venäläinen, Ari ja Tuomenvirta Heikki, 1998. Arvio ilmaston läm- penemisen vaikutuksesta teiden talvikunnossapidon kustannuksiin. 19 s.

1999:

1. Mälkki, Anssi, 1999. Near earth electron environment modelling tool user/software requirements document. 43 p.

2. Pulkkinen, Antti, 1999. Geomagneettisesti indusoituvat virrat Suomen maakaasuverkostossa. 46 s.

3. Venäläinen, Ari, 1999. Talven lämpötilan ja maanteiden suolauksen välinen riippuvuus Suomessa.16 s.

4. Koskinen, H., Eliasson, L., Holback, B., Andersson, L., Eriksson, A., Mälkki, A., Nordberg, O., Pulkkinen, T., Viljanen, A., Wahlund, J.-E., Wu, J.-G., 1999. Space weather and interactions with scacecraft : spee final report. 191 p.

2000:

1 Solantie, Reijo ja Drebs, Achim, 2000. Kauden 1961 - 1990 lämpöoloista kasvukautena alustan vaikutus huomioiden, 38 s.

2. Pulkkinen, Antti, Viljanen, Ari, Pirjola, Risto, and Bear working group, 2000. Large geomagnetically induced currents in the Finnish high-voltage power system. 99 p.

3. Solantie, R. ja Uusitalo, K., 2000. Patoturvallisuuden mitoitussadannat: Suomen suurimpien 1, 5 ja 14 vrk:n piste- ja aluesadantojen analysointi vuodet 1959 - 1998 kattavasta aineistosta. 77 s.

4. Tuomenvirta, Heikki, Uusitalo, Kimmo, Vehviläinen, Bertel, Carter, Timothy, 2000. Ilmastonmuutos, mitoitussadanta ja patoturvallisuus: arvio sadannan ja sen ääriarvojen sekä lämpötilan muutoksista Suomessa vuoteen 2100. 65 s.

5. Viljanen, Ari, Pirjola, Risto and Tuomi, Tapio, 2000. Abstracts of the URSI XXV national convention on radio science. 108 p.

6. Solantie, Reijo ja Drebs, Achim, 2000. Keskimääräinen vuoden ylin ja alin lämpötila Suomessa 1961 - 90. 31 s.

7. Korhonen, Kimmo, 2000. Geomagneettiset mallit ja IGRF-appletti. 85 s.

2001:

1. Koskinen, H., Tanskanen, E., Pirjola, R., Pulkkinen, A., Dyer, C., Rodgers, D., Cannon, P., Mandeville, J.-C. and Boscher, D., 2001. Space weather effects catalogue. 41 p.

2. Koskinen, H., Tanskanen, E., Pirjola, R., Pulkkinen, A., Dyer, C., Rodgers, D., Cannon, P., Mandeville, J.-C. and Boscher, D., 2001. Rationale for a european space weather programme. 53 p.

3. Paatero, J., Valkama, I., Makkonen, U., Laurén, M., Salminen, K., Raittila, J. and Viisanen, Y., 2001. Inorganic components of the ground-level air and meteorological parameters at Hyytiälä, Finland during the BIOFOR project 1998-1999. 48 p.

4. Solantie, Reijo, Drebs, Achim, 2001. Maps of daily and monthly minimum temperatures in Finland for June, July, and August 1961-1990, considering the effect of the underlying surface. 28 p.

5. Sahlgren, Vesa, 2001. Tuulikentän alueellisesta vaihtelusta Längelmävesi-Roine -järvialueella. 33 s.

6. Tammelin, Bengt, Heimo, Alain, Leroy, Michel, Rast, Jacques and Säntti, Kristiina, 2001. Meteorological measurements under icing conditions : EUMETNET SWS II project. 52 p.

2002:

1. Solantie, Reijo, Drebs, Achim, Kaukoranta, Juho-Pekka, 2002. Lämpötiloja eri vuodenaikoina ja eri maastotyypeissä Alajärven Möksyssä. 57 s.

2. Tammelin, Bengt, Forsius, John, Jylhä, Kirsti, Järvinen, Pekka, Koskela, Jaakko, Tuomenvirta, Heikki, Turunen, Merja A., Vehviläinen, Bertel, Venäläinen, Ari, 2002. Ilmastonmuutoksen vaikutuksia energiantuotantoon ja lämmitysenergian tarpeeseen. 121 s.

2003:

1. Vajda, Andrea and Venäläinen, Ari, 2003. Small-scale spatial variation of climate in northern Finland. 34 p.

2. Solantie, Reijo, 2003. On definition of ecoclimatic zones in Finland. 44 p.

3. Pulkkinen, T.I., 2003. Chapman conference on physics and modelling of the inner magnetosphere Helsinki, Finland, August 25 -29, 2003. Book of abstracts. 110 p.

4. Pulkkinen, T. I., 2003. Chapman conference on physics and modelling of the inner magnetosphere Helsinki, Finland, August 25 -29, 2003. Conference program. 16 p.

5. Merikallio, Sini, 2003. Available solar energy on the dusty Martian atmosphere and surface. 84 p.

6. Solantie, Reijo, 2003. Regular diurnal temperature variation in the Southern and Middle boreal zones in Finland in relation to the production of sensible heat. 63 p.

2004:

1. Solantie, Reijo, Drebs, Achim and Kaukoranta, Juho-Pekka, 2004. Regular diurnal temperature variation in various landtypes in the Möksy experimental field in summer 2002, in relation to the production of sensible heat. 69 p.

2. Toivanen, Petri, Janhunen, Pekka and Koskinen, Hannu, 2004. Magnetospheric propulsion (eMPii). Final report issue 1.3. 78 p.

3. Tammelin, Bengt et al., 2004. Improvements of severe weather measurements and sensors - EUMETNET SWS II project. 101 p.

4. Nevanlinna, Heikki, 2004. Auringon aktiivisuus ja maapallon lämpötilan vaihtelut 1856 - 2003. 43 s.

5. Ganushkina, Natalia and Pulkkinen, Tuija, 2004. Substorms-7: Proceedings of the 7th International Confrence on Substorms. 235 p.

6. Venäläinen, Ari, Sarkkula, Seppo, Wiljander, Mats, Heikkinen, Jyrki, Ervasto, Erkki, Poussu, Teemu ja Storås, Roger, 2004. Espoon kaupungin talvikunnossapidon sääindeksi. 17 s.

7. Paatero, Jussi and Holmen, Kim (eds.), 2004. The First Ny-Ålesund - Pallas-Sodankylä atmospheric research workshop, Pallas, Finland 1 - 3 March 2004 - Extended abstracts. 61 p.

8. Holopainen, Jari, 2004. Turun varhainen ilmastollinen havaintosarja. 59 s.

2005:

1. Ruuhela, Reija, Ruotsalainen, Johanna, Kangas, Markku, Aschan, Carita, Rajamäki, Erkki, Hirvonen, Mikko ja Mannelin, Tarmo, 2005. Kelimallin kehittäminen talvijalankulun turvallisuuden parantamiseksi. 47 s.

2. Laurila, Tuomas, Lohila, Annalea, Tuovinen, Juha-Pekka, Hatakka, Juha, Aurela, Mika, Thum, Tea, Walden, Jari, Kuronen, Pirjo, Talka, Markus, Pesonen, Risto, Pihlatie, Mari, Rinne, Janne, Vesala, Timo, Ettala, Matti, 2005. Kaatopaikkojen kaasupäästöjen ja haihdunnan mikrometeorologisten mittausmenetelmien kehittäminen (MIKROMETKAA). Tekesin Streams -ohjelman hankken loppuraportti. 34 s. (Ei julkaistu - Not published)

3. Siili, Tero, Huttunen, Emilia, Koskinen, Hannu ja Toivanen, Petri (toim.), 2005. Kymmenes Suomen avaruustutkijoiden kokous (FinCospar) Kokousjulkaisu. 57 s.

4. Solantie, Reijo and Pirinen, Pentti, 2005. Diurnal temperature variation in inversion situations. 34 s.

5. Venäläinen, Ari, Tuomenvirta, Heikki, Pirinen, Pentti and Drebs, Achim, 2005. A basic Finnish climate data set 1961 - 2000 - description and illustrations. 24 p.

6. Tammelin, Bengt, Säntti, Kristiina, Dobech, Hartwig, Durstewich, Michel, Ganander, Hans, Kury, Georg, Laakso, Timo, Peltola, Esa, Ronsten, Göran, 2005. Wind turbines in icing environment: improvement of tools for siting, certification and operation - NEW ICETOOLS. 127 p.

2006:

1. Mälkki, Anssi, Kauristie, Kirsti and Viljanen Ari, 2006. Auroras Now! Final Report, Volume I. 73 p.

2. Pajunpää, K. and Nevanlinna, H. (eds), 2006. Nurmijärvi Geophysical Observatory : Magnetic results 2003. 47 p.

3. Pajunpää, K. and Nevanlinna, H. (eds), 2006. Nurmijärvi Geophysical Observatory : Magnetic results 2004. 47 p.

4. Pajunpää, K. and Nevanlinna, H. (eds), 2006. Nurmijärvi Geophysical Observatory : Magnetic results 2005. 49 p.

5. Viljanen, A. (toim.), 2006. Sähkömagnetiikka 2006. Tiivistelmät - Abstracts. 30 s.

6. Tuomi, Tapio J. & Mäkelä, Antti, 2006. Salamahavainnot 2006 - Lightning observations in Finland, 2006. 39 p.

7. Merikallio, Sini, 2006. Preliminary report of the analysis and visualisation software for SMART-1 SPEDE and EPDP instruments. 70 p.

8. Solantie, Reijo, Pirinen, Pentti, 2006. Orografian huomioiminen loka- huhtikuun sademäärien alueellisissa analyyseissä. 34 s.

9. Ruosteenoja, Kimmo, Jylhä, Kirsti, Räisänen, Petri, 2006. Climate projections for the Nordic CE project - an analysis of an extended set of global regional climate model runs. 28 p.

10. Merikallio, Sini, 2006. Analysis and visualisation software for DEMETER Langmuir Probe instrument. 31 p.

2007:

1. Solantie, Reijo, Järvenoja, Simo, Pirinen, Pentti, 2007. Keskimääräisten kuukauden minimilämpötilojen alueellinen jakauma kautena 1992 - 2005 Suomessa sekä muutos kaudesta 1961 -

1990. 59 s.

2. Pulkkinen, Tuija, Hari, Ari-Matti, Haukka, Harri, Leinonen, Jussi, Toivanen, Petri, Koskinen, Hannu, André, Mats, Balasis, Georgios, Boscher, Daniel, Dandouras, Iannis, Grande, Mauel, De Keyser, John, Glassmeier, Karl-Heinz, Hapgood, Mike, Horne, Richard, Ivchenko, Nikolay, Santolik, Ondrej, Torkar, Klaus; Trotignon, Jean Gabriel, Vennerstrøm, Susanne, 2007. Waves and acceleration of relativistic particles (WARP). 36 p.

3. Harri, A-M., Leinonen, J., Merikallio, S., Paton, M., Haukka, H., Polkko, J., Linkin, V., Lipatov, V., Pichkadze, K., Polyakov, A., Uspensky, M., Vasquez, L., Guerrero, H., Crisp, D., Haberle, R., Calcutt, S., Wilson, C., Taylor, P., Lange, C., Daly, M., Richter, L., Jaumann, R., Pommereau, J-P., Forget, F., Lognonne, Ph., Zarnecki, J., 2007. MetNet - In situ observational network and orbital platform to investigate the Martian environment. 35 p.

4. Venäläinen, Ari, Saku, Seppo, Kilpeläinen, Tiina, Jylhä, Kirsti, Tuomenvirta, Heikki, Vajda, Andrea, Räisänen, Jouni, Ruosteenoja, Kimmo, 2007. Sään ääri-ilmiöistä Suomessa. 81 s.

5. Tuomi, Tapio J. & Mäkelä, Antti, 2007. Salamahavainnot 2007 - Lightning observations in Finland, 2007. 47 p.

6. Pajunpää, K. and Nevanlinna, H. (eds), 2007. Nurmijärvi Geophysical Observatory : Magnetic results 2006. 49 p.

2008:

1. Pajunpää, K. and Nevanlinna, H. (eds), 2008. Nurmijärvi Geophysical Observatory : Magnetic results 2007. 49 p.

2. Verronen, Pekka T. (ed), 2008. 1st international HEPPA workshop 2008, Book of abstracts. 81 p.

3. Gregow, Hilppa, Venäläinen, Ari, Laine, Mikko, Niinimäki, Niina, Seitola, Teija, Tuomenvirta, Heikki, Jylhä, Kirsti, Tuomi, Tapio ja Mäkelä, Antti, 2008. Vaaraa aiheuttavista sääilmiöistä Suomen muuttuvassa ilmastossa. 99 s.

4. Tuomi, Tapio J. & Mäkelä, Antti, 2008. Salamahavainnot 2008 - Lightning observations in Finland, 2008. 49 p.

5. Heino, Raino and Tolonen-Kivimäki, Outi (eds), 2008. Finnish national report on systematic observations for climate - 2008. 27 p. 6. Paatero, Jussi et al., 2008. Effects of Kola air pollution on the environment in the western part of the Kola peninsula and Finnish Lapland : final report. 26 p.

2009:

1. Nevanlinna, H., 2009. Geomagnetismin ABC-kirja. 204 s.

2. Nevanlinna, H. (toim.), 2009. Ilmatieteen laitos 170 vuotta, 1838 - 2008. 69 s.

3. Nevanlinna, Heikki, 2009. Revontulihavainnot Suomessa 1748 - 2009. 88 s.

4. Jylhä, K., Ruosteenoja, K., Räisänen, J., Venäläinen, A., Tuomenvirta, H., Ruokolainen, L., Saku, S. ja Seitola, T., 2009. Arvioita Suomen muuttuvasta ilmastosta sopeutumistutkimuksia varten. ACCLIM-hankkeen raportti 2009. 102 p.

5. Mäkelä, Antti & Tuomi, Tapio, J., 2009. Salamahavainnot 2009 - Lightning observations in Finland, 2009. 51 p.

6. Verronen, Pekka (ed.), 2009. 5th International Atmospheric Limb Conference and Workshop : Book of abstracts. 92 p.

7. Pajunpää, K. and Nevanlinna, H. (eds), 2009. Nurmijärvi Geophysical Observatory : Magnetic results 2008. 48 p.

8. Kersalo, Juha and Pirinen, Pentti (eds), 2009. Suomen maakuntien ilmasto. 185 s.

2010:

1. Rauhala, Jenni & Mäntyniemi, Päivi, 2010. Luonnononnettomuuksien vaikutus ja niihin vaikuttaminen. (valmisteilla).

2. Pilli-Sihvola, K. Löwendahl, E., Ollikainen, M., van Oort, B., Rummukainen, M. & Tuomenvirta, H., 2010. Survey on the use of climate scenarios and climate change research information in decision making in Finland, Sweden and Norway. Report for the project Climate change adaption in Norway, Sweden and Finland - do research, policy and practice meet? (CARePol). 57 p.

3. Pajunpää, K. and Nevanlinna, H. (eds), 2010. Nurmijärvi Geophysical Observatory : Magnetic results 2009. 48 p.

4. Luomaranta, A., Haapala, J., Gregow, H., Ruosteenoja, K., Jylhä, K. and Laaksonen, A. 2010. Itämeren jääpeitteen muutokset vuoteen 2050 mennessä. 23 s.

5. Mäkelä, Antti, 2010. Salamahavainnot 2010 - Lightning observations in Finland, 2010. 50 p.

2011:

1. Saku, Seppo et al., 2011. Äärilämpötilojen alueellinen vaihtelu Suomessa. (valmisteilla)

2. Pajunpää, K. and Nevanlinna, H. (eds), 2011. Nurmijärvi Geophysical Observatory : Magnetic results 2010. 49 p.

3. Virta, Hanna et al., 2011. Ilmastonmuutoksen ääri-ilmiöihin liittyvän riskienhallinnan kustannushyötyanalyysi osana julkista päätöksentekoa (IRTORISKI). 97 s.

4. Nevanlinna, H. 2011. Magneettiset havainnot Helsingin magneettis-meteorologisessa observatoriossa, 1844-1910. 54 s.

5. Hilppa Gregow, Kimmo Ruosteenoja, Ilkka Juga, Sigbritt Näsman, Miika Mäkelä, Mikko Laapas, Kirsti Jylhä, 2011. Lumettoman maan routaolojen mallintaminen ja ennustettavuus muuttuvassa ilmastossa. 45 s.

6. Jylhä, Kirsti et al. (valmisteilla)

7. Mäkelä, Antti, 2011. Salamahavainnot 2011 - Lightning observations in Finland, 2011. (valmisteilla)

8. Riihelä, A., Lahtinen, P., Hakala, T. 2011. The Radiation, Snow Characteristics and Albedo at Summit (RASCALS) expedition report. 48 p.

Ilmatieteen laitos
Erik Palménin aukio 1, Helsinki
tel. (09) 19 291
www.fmi.fi

ISBN 978-951-697-759-4 (nid.)
ISBN 978-951-697-760-0 (pdf)
ISSN 0782-6079
Unigrafia
Helsinki 2011